Bibliographical reference

Sensorless Electroacoustic Absorbers Through Synthesized Impedance Control for Damping Low-Frequency Modes in Cavities, Romain Boulandet, Etienne Rivet and Hervé Lissek, Acta Acustica **vol. 102** (Number 4), 2016, pp. 696-704

DOI

https://doi.org/10.3813/AAA.918986

Acta Acustica united with Acustica
Vol. 102 (2016) 696 – 704

DOI 10.3813/AAA.918986

Sensorless Electroacoustic Absorbers Through Synthesized Impedance Control for Damping Low-Frequency Modes in Cavities

Romain Boulandet, Etienne Rivet, Hervé Lissek
Laboratoire de Traitement des Signaux LTS2, Ecole Polytechnique Fédérale de Lausanne, Station 11, 1015, Lausanne, Switzerland. herve.lissek@epfl.ch

Summary
This paper presents a concept of sensorless electroacoustic absorber for damping the low-frequency modes in a cavity such as a duct or a room. Taking advantage of the reciprocity of the voice coil transducer, it is shown that a synthetic electrical admittance can be designed so that the loudspeaker diaphragm is matched to a target specific acoustic impedance. This electroacoustic device provides a relatively broadband sound absorption that can be used to dampen room modes regardless of the sound field in which the loudspeaker is located. A digital filter is used to replicate the frequency response of the synthetic load, and a voltage-controlled current source is needed so that the filter is seen as an electrical admittance. Unlike previous attempts to implement the synthetic load using an electrical network, greater flexibility and accuracy can be obtained. Experimental results confirmed the validity of this sensorless electroacoustic absorber (SEA) in a 1D sound field, showing that the dynamic range of the sound pressure level in a duct can be reduced by 15 dB from 50 Hz to 300 Hz compared to a hard surface panel. A discussion on the strengths and limitations of this concept is provided, in particular with a view to employing SEAs for modal equalization in actual listening rooms.

PACS no. 43.38.Dv, 43.20.Ks

1. Introduction

Room modes can significantly impair the quality of sound diffusion in small listening rooms, where the modal behaviour dominates typically between 20 Hz to 200 Hz [1]. These modes are mainly characterized by an uneven spatial distribution of the acoustic energy in the room that can hardly be avoided, even with an "optimal" arrangement of loudspeakers and listening positions [2]. In terms of auditory perception, the decay times associated to each mode may have a direct impact on the sound rendering at low frequencies, in a similar fashion to the reverberation in the middle-high frequency range [3]. These modal decay times depend on the wall impedance and are known to significantly impact the listening experience [4]. It is therefore crucial to employ low-frequency absorbing devices to provide the best listening experience over the entire audio range. Bass traps and Helmholtz resonators are commonly used solutions, but due to their narrow bandwidth of absorption the target frequency decade from 20 Hz to 200 Hz can hardly be covered using a single absorber [2]. The damping of one single room resonance may not be perceptually audible in the presence of other strong modal resonances, and broadband acoustic absorbers should therefore be considered.

The attenuation of low-frequency modes in small rooms can also be achieved from electroacoustic transducers, where a loudspeaker diaphragm is advantageously employed as a tunable membrane absorber. Indeed, the mechanical resonance of conventional electrodynamic loudspeakers generally ranges between 20 Hz and 200 Hz, i.e. below the Schroeder frequency for most listening rooms [1]. For normal sound incidence, a perfect impedance matching can be obtained at the loudspeaker resonance frequency, only through mechanical dissipation and resistive heating. [5, 6]. As for bass traps, however, the bandwidth of efficient sound absorption is very limited due to the quality factor of the loudspeaker mechanical resonance. The sound absorption coefficient of the loudspeaker diaphragm can be improved by connecting a simple resistor to its input terminals, or a more complex electrical network such as resonant RLC circuits [7, 8, 9]. A microphone and a velocity sensor can even be used in combination to a feedback controller to further increase the bandwidth of efficient absorption at the loudspeaker diaphragm [5, 10, 11, 12], but it is generally accompanied with an increased cost and complexity. In the mid 2000's, moreover, a technique for damping of the resonance of a single DOF system was proposed by Fleming *et al.* using an electrodynamic actuator connected to a synthetic electrical

Received 21 July 2015,
accepted 3 June 2016.

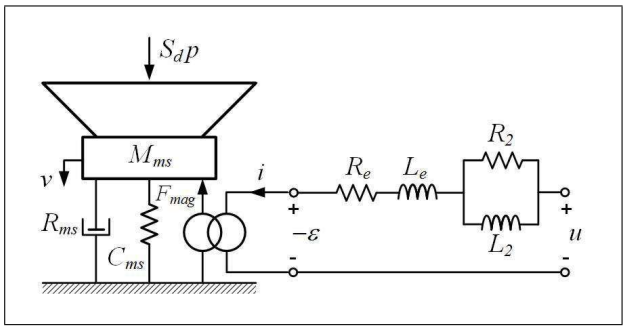

Figure 1. Scheme of an electrodynamic loudspeaker, where the current $\underline{i}$ is defined as going into the electrical port of the transducer and the velocity $\underline{v}$ is defined as going into the mechanical port of the transducer.

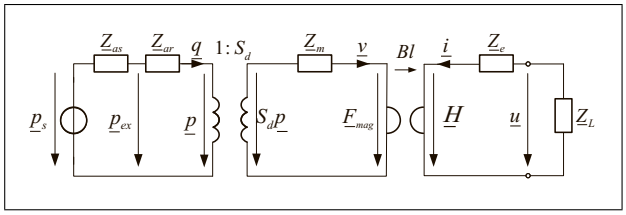

Figure 2. Analogous electrical circuit representation of the electrodynamic loudspeaker connected to an electrical load $\underline{Z}_L$ and subject to an external sound field.

admittance [13]. Their approach was then applied to optimally control the resonant sound field in a duct [8], where an optimal shunt admittance was derived through standard methods such as linear quadratic regulator (LQR) or $\mathcal{H}_2$. While this approach leads to optimum damping of the duct modes in a relatively wide frequency range, it is not robust to changes in the sound field or the location of the control loudspeaker.

Recently, the concept of electroacoustic absorber (EA) was introduced as a practical means to achieve sound absorption at low frequencies [6]. In this technique, a shunt electrical impedance is derived from a model of the loudspeaker, so as to achieve impedance matching at the diaphragm. Although this shunt impedance can be expressed theoretically as a network using resistors and inductors, its practical implementation can hardly be achieved using actual electrical components. This is partly due to the non-ideal behaviour of the coil and the parasitic resistances of the inductors used in the electrical network which must be neutralized with negative counterparts. Any mismatch between the loudspeaker model parameters and the network may then affect the closed loop stability [14]. Nevertheless, this work has brought a new perspective on the use of a loudspeaker as a stand-alone electroacoustic absorber.

This paper presents a concept of sensorless electroacoustic absorber (SEA) inspired by [6] and [8]. Taking advantage of the reciprocity of the voice coil transducer, it is shown that a shunt electrical admittance can be designed so that the loudspeaker diaphragm is matched to a target specific acoustic impedance, regardless of the sound field in which the loudspeaker is located. The remainder of the paper is organized as follows. The model-based method used to derive the complex, frequency-dependent electrical admittance leading to the desired specific acoustic impedance is given in Section 2. Computed and measured results showing the acoustic absorption capability of the SEA are provided in Section 3, including experimental results on modal damping in a duct. A discussion on strengths and limitations of this concept is given in Section 4, in particular with a view to using SEAs for modal equalization in actual listening rooms.

2. Design of a sensorless electroacoustic absorber

This section provides the theoretical background on the characteristics of the electrodynamic loudspeaker, and specifies how it can be employed as a SEA. A lumped parameter model is used in the following assuming time-harmonic dependence $p(t) = \mathrm{Re}[\underline{p}\exp(\mathrm{j}\omega t)]$ and linear behaviour. Otherwise, some of the model parameters would need to be considered as time-varying nonlinear functions of the input variables [15, 16], which might also have consequences on the characteristics of the electroacoustic absorber [17].

2.1. Model of the electrodynamic loudspeaker

Figure 1 gives a schematic representation of the electrodynamic loudspeaker. The equation of motion of the loudspeaker diaphragm can be written as

$$S_d\,\underline{p} = \left(\mathrm{j}\omega M_{ms} + R_{ms} + \frac{1}{\mathrm{j}\omega C_{ms}}\right)\underline{v} + \underline{F}_{mag}, \qquad (1)$$

where $\underline{p}$ is the total pressure at the diaphragm due to incident and reflected sound waves, $\underline{v}$ is the diaphragm velocity, $\underline{i}$ is the current flowing through the coil, S_d is the effective piston area of the diaphragm radiating surface, M_{ms} and R_{ms} are the equivalent mass and mechanical resistance of the moving bodies, and C_{ms} is the equivalent mechanical compliance accounting for the surround suspension and the spider; $\underline{F}_{mag} = Bl\underline{i}$ represents the Laplace force resulting from the magnetic field action on a free moving charge (current), where B is the magnetic flux density (in T) and l is the total length (in m) of the conductor.

The governing equation of the electrical dynamics can be written as [18]

$$\underline{u} = \left(\mathrm{j}\omega L_e + R_e + \frac{\mathrm{j}\omega L_2 R_2}{\mathrm{j}\omega L_2 + R_2}\right)\underline{i} + \varepsilon, \qquad (2)$$

where $\underline{u}$ is the input voltage at the electrical terminals, L_e and R_e are the self inductance and dc resistance of the coil, respectively, L_2 and R_2 represent the para-inductance and resistance due to eddy currents in the voice coil transducer, respectively, and $\underline{\varepsilon} = -Bl\,\underline{v}$ is the back electromotive force induced within the coil during motion.

Let us consider the case where the loudspeaker is enclosed in a cabinet of volume V_b, resulting in a total mechanical compliance $C_{mc} = C_{ms}\,(1 + \rho c^2 S_d^2 C_{ms}/V_b)^{-1}$,

where $\rho = 1.2\,\mathrm{kg\ m^{-3}}$ is the density of air and $c = 345$ m s^{-1} is the speed of sound in air. C_{mc} is now substituted to C_{ms} in Equation (1), and Equations (1)–(2) can then be expressed as

$$\begin{cases} S_d\,\underline{p} = \underline{Z}_m\,\underline{v} + Bl\,\underline{i}, \\ \underline{u} = \underline{Z}_e\,\underline{i} - Bl\,\underline{v}, \end{cases} \tag{3}$$

where $\underline{Z}_m = \mathrm{j}\omega M_{ms} + R_{ms} + (\mathrm{j}\omega C_{mc})^{-1}$ is the mechanical impedance of the closed-box loudspeaker, and $\underline{Z}_e = \mathrm{j}\omega L_e + R_e + \mathrm{j}\omega L_2 R_2\,(\mathrm{j}\omega L_2 + R_2)^{-1}$ is the blocked electrical impedance of the voice coil including eddy currents. Figure 2 gives the analogous electrical circuit representation of the electrodynamic loudspeaker. The part on the left-hand side of Figure 2 accounts for an external sound field, including a pressure source $\underline{p}_s$ of internal impedance $\underline{Z}_{as}$ and an acoustic radiation impedance $\underline{Z}_{ar}$ which depends on the geometry of the enclosure, the volume of the room in which the loudspeaker radiates and its location therein. Without loss of generality, $\underline{Z}_{ar}$ is included into $\underline{Z}_m$ in the form of a radiation mass and added resistance [19].

2.2. Connection to a shunt electrical impedance

Let us now consider an electrical load represented by the complex impedance $\underline{Z}_L$ connected to the transducer terminals, as shown in Figure 2. When the coil is vibrating with velocity $\underline{v}$, the current flowing through the electrical circuit closed by $\underline{Z}_L$ is given by

$$\underline{i} = -\frac{1}{\underline{Z}_e + \underline{Z}_L}\underline{\varepsilon} = \frac{Bl}{\underline{Z}_e + \underline{Z}_L}\underline{v}. \tag{4}$$

The specific acoustic impedance of the loudspeaker diaphragm [1] can therefore be derived by substituting Equation (4) into Equations (3) as

$$\underline{Z}_s = \frac{\underline{p}}{\underline{v}} = \frac{\underline{Z}_m}{S_d} + \frac{(Bl)^2}{S_d(\underline{Z}_e + \underline{Z}_L)}. \tag{5}$$

showing how the complex impedance $\underline{Z}_L$ may change the diaphragm specific acoustic impedance.

2.3. Sound absorption coefficient and bandwidth

For plane waves under normal incidence [22], the sound absorption coefficient α of the loudspeaker diaphragm can be obtained from Equation (5) as

$$\alpha = 1 - \left|\frac{\underline{Z}_s - \rho c}{\underline{Z}_s + \rho c}\right|^2. \tag{6}$$

The bandwidth of efficient sound absorption is the frequency range over which the total sound energy in front of the diaphragm is less than twice the total sound energy in the case of ideal acoustic impedance matching, i.e. $\underline{Z}_s = \rho c$ (or $\alpha = 1$). This criterion corresponds to a sound absorption coefficient $\alpha \geq 0.83$ [2]. Note that the sound absorption coefficient given in Equation (6) should not be confused with the total absorbed energy $A = S\alpha$, usually called "absorption" in the case of an absorber which is large compared to the wavelength and has an effective area S.

2.4. Target specific acoustic impedance

When the loudspeaker is disposed at the termination of a waveguide and subject to plane waves under normal incidence, the condition for ideal impedance matching at the loudspeaker diaphragm is $\underline{Z}_s = \rho c$, if the duct section is approximately S_d [26]. However, this goal can hardly be achieved over the whole frequency range of interest due to the bandpass response of the loudspeaker, as shown in Equation (5). Achieving $\underline{Z}_s = \rho c$ at the diaphragm would require to cancel the effects of the reactive components C_{mc} and M_{ms} in the loudspeaker system through negative counterparts. Therefore, the target diaphragm specific impedance is defined in the following as a second-order system

$$\underline{Z}_{st} = \frac{R_{mt}}{S_d} + \mathrm{j}\left(\frac{\omega M_{mt}}{S_d} - \frac{1}{\omega S_d C_{mt}}\right), \tag{7}$$

where R_{mt}, M_{mt} and C_{mt} are the target mechanical resistance, mass and effective compliance, respectively.

The bandwidth B of efficient sound absorption defined in 2.3 can be derived by substituting Equation (7) into Equation (6) and solving $\alpha \geq 0.83$:

$$B = \frac{|R_{mt} + \rho c S_d|}{2\pi M_{mt}}\sqrt{\frac{\left(\sqrt{2}-1\right)^2 - \left(\frac{R_{mt}-\rho c S_d}{R_{mt}+\rho c S_d}\right)^2}{1-\left(\sqrt{2}-1\right)^2}} \tag{8}$$

only valid for

$$\left|\, R_{mt} - \sqrt{2}\,\rho c S_d \,\right| \leq S_d\sqrt{\rho^2 c^2 - 1}.$$

Note that assuming $R_{mt} = \rho c S_d$ (ideal impedance matching), the second term in the numerator in the square root vanishes and Equation (8) leads to

$$B = \rho c S_d/(\pi M_{mt})\sqrt{\frac{\left(\sqrt{2}-1\right)^2}{1-\left(\sqrt{2}-1\right)^2}},$$

showing that the ratio S_d/M_{mt} is a significant parameter for extending the bandwidth.

[1] defined as the relationship between the acoustic pressure applied to the diaphragm and the resulting particle velocity in the direction of that pressure at its point of application

[2] For normal sound incidence, the total (incident + reflected) sound energy is proportional to $(1 + \underline{r})^2$. In the ideal case: $(1 + \underline{r})^2 = 1$. In the threshold case (bounds of the bandwidth): $(1 + \underline{r}_{min})^2/2 = 1$, thus $\alpha_{min} = 0.83$.

Table I. Physical parameters measured on a Monacor SPX-30M loudspeaker loaded by a rear sealed enclosure of volume $V_b = 0.96\ \mathrm{dm}^3$.

Parameter	Notation	Value	Unit
dc resistance	R_e	6.4	Ω
Voice coil inductance	L_e	0.23	mH
Resistance due to eddy currents	R_2	1.6	Ω
Para-inductance of the voice coil	L_2	0.23	mH
Transduction coefficient	Bl	3.3	$\mathrm{N\,A^{-1}}$
Moving mass	M_{ms}	2.67	g
Mechanical resistance	R_{ms}	0.49	$\mathrm{N\,s\,m^{-1}}$
Equivalent mechanical compliance	C_{mc}	0.38	$\mathrm{mm\,N^{-1}}$
Effective piston area	S_d	32	cm^2
Equivalent volume	V_{as}	1.78	dm^3
Resonance frequency	f_{EA}	158	Hz

2.5. Derivation of the shunt electrical admittance

Combining now Equations (5) and (7), the closed form expression of the load electrical impedance that should be connected to assign $\underline{Z}_{st}$ at the loudspeaker diaphragm can be derived as

$$\underline{Z}_L = \frac{\underline{u}}{\underline{i}} = -\underline{Z}_e + \frac{(Bl)^2}{S_d \underline{Z}_{st} - \underline{Z}_m}. \tag{9}$$

As can be seen in Equation (9), the complex impedance $\underline{Z}_L$ comprises a negative term $-\underline{Z}_e$ needed to cancel the coil electrical impedance and an additional term used to change the motional impedance of the loudspeaker. However, Equation (9) would not lead to a proper transfer function and cannot be directly implemented on a digital platform. The reciprocal of Equation (9) should be considered instead, so that the functional relationship to be assigned between current and voltage cannot increase unbounded as the frequency approaches infinity. The electrical load to be implemented is therefore expressed as an electrical admittance (in Ω^{-1})

$$\underline{Y}_L(\omega) = -\frac{\sum_{i=0}^{3} (\mathrm{j}\omega)^i\, a_i}{\sum_{i=1}^{4} (\mathrm{j}\omega)^i\, b_i}, \tag{10}$$

where

$$\begin{cases} a_3 = L_2(M_{ms} - M_{mt}) \\ a_2 = L_2(R_{ms} - R_{mt}) + R_2(M_{ms} - M_{mt}) \\ a_1 = L_2(1/C_{mc} - 1/C_{mt}) + R_2(R_{ms} - R_{mt}) \\ a_0 = R_2(1/C_{mc} - 1/C_{mt}) \end{cases}$$

and

$$\begin{cases} b_4 = a_3\, L_e \\ b_3 = a_2\, L_e + a_3\, R_e + R_2 L_2 (M_{ms} - M_{mt}) \\ b_2 = a_1\, L_e + a_2\, R_e + R_2 L_2 (R_{ms} - R_{mt}) + L_2 (Bl)^2 \\ b_1 = a_0\, L_e + a_1\, R_e + R_2 L_2 (1/C_{mc} - 1/C_{mt}) + R_2 (Bl)^2 \\ b_0 = a_0\, R_e \end{cases}$$

3. Results

This section presents simulation and experimental results intended to show the acoustic performance for normal sound incidence of a SEA developed from the Monacor SPX-30M loudspeaker. The electromechanical parameters of the loudspeaker were measured from the method described in [20] and are listed in Table I, where the resonance frequency and the equivalent mechanical compliance account for the combined effects of the loudspeaker and an enclosure of volume $V_b = 0.96\ \mathrm{dm}^3$.

3.1. Numerical simulation

Table II summarizes the setting parameters and the expected control results in terms of bandwidth and maximum sound absorption coefficient at resonance. Note that each setting was defined so as to preserve the resonance frequency f_{EA} of the SEA, i.e. $C_{mt} M_{mt} = C_{mc} M_{ms}$. Referring to Table II, the baseline configuration A corresponds to the situation without application of any electrical load (open circuit). In case B, the target mechanical resistance is set to an optimal value ($R_{mt} = \rho c S_d$) for ideal acoustic impedance matching at $f_0 = f_{EA}$, while the mass and compliance of the loudspeaker diaphragm are not modified. This configuration is equivalent to a loudspeaker shunted by a resistor, the value of which is $R_{opt} = (Bl)^2/(\rho c S_d - R_{ms}) - R_e$ for ideal impedance matching at the resonance of the loudspeaker, as shown in [6]. Medium acoustic absorption is targeted in case C for which the mechanical resistance is half the optimum value ($\rho c S_d/2$), the moving mass is halved and the effective compliance is doubled compared to the passive case (case A). Case D corresponds to the situation targeting the optimal value of mechanical resistance ($R_{mt} = \rho c S_d$), while halving the moving mass and doubling the effective compliance. Thus, the bandwidth is expected to double in comparison with case B.

Figure 3 illustrates the frequency response of the specific acoustic impedance $\underline{Z}_s$ computed with the control settings listed in Table II, and the corresponding sound absorption coefficient. Without control (open circuit, case A), the diaphragm of the speaker has a maximum absorption coefficient of about 0.8 at resonance. As expected, connecting an electrical resistance to the loudspeaker terminals increases the total acoustic resistance, thus improving the sound absorption coefficient of the diaphragm (see case B). On the other hand, reducing the reactive components in the loudspeaker diaphragm can increase the bandwidth of efficient acoustic absorption (see case D). Fig-

Table II. Setting parameters and computed control results.

Case	Setting parameters			Expected control results		
	M_{mt}	R_{mt}	C_{mt}	f_0	α_{max}	B
A	M_{ms}	R_{ms}	C_{mc}	158.0 Hz	0.79	–
B	M_{ms}	$\rho c S_d$	C_{mc}	158.0 Hz	1	71.9 Hz
C	$\frac{1}{2} M_{ms}$	$\frac{1}{2} \rho c S_d$	$2\,C_{mc}$	158.0 Hz	0.89	64.0 Hz
D	$\frac{1}{2} M_{ms}$	$\rho c S_d$	$2\,C_{mc}$	158.0 Hz	1	143.8 Hz

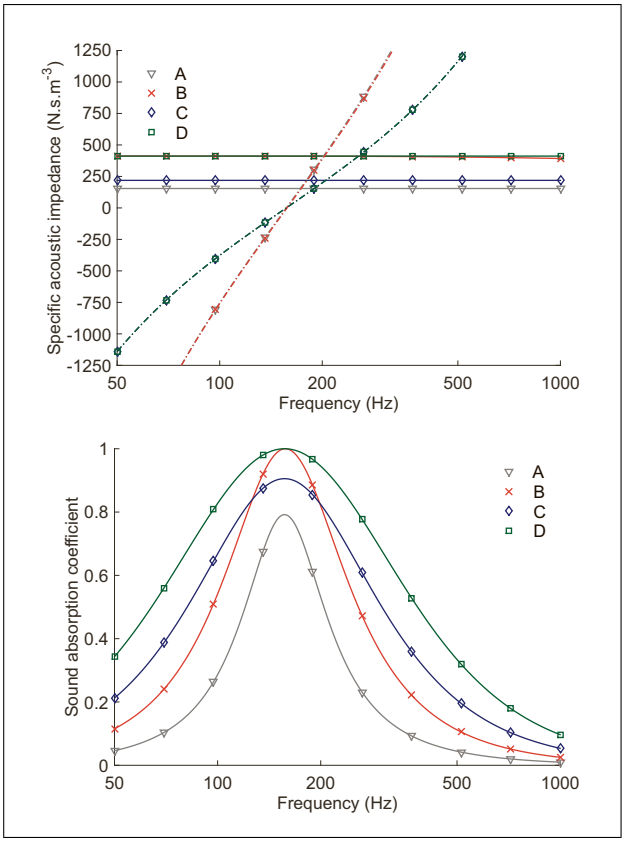

Figure 3. Real part (—) and imaginary part (- - -) of the computed specific acoustic impedance (top) and corresponding sound absorption coefficient (bottom).

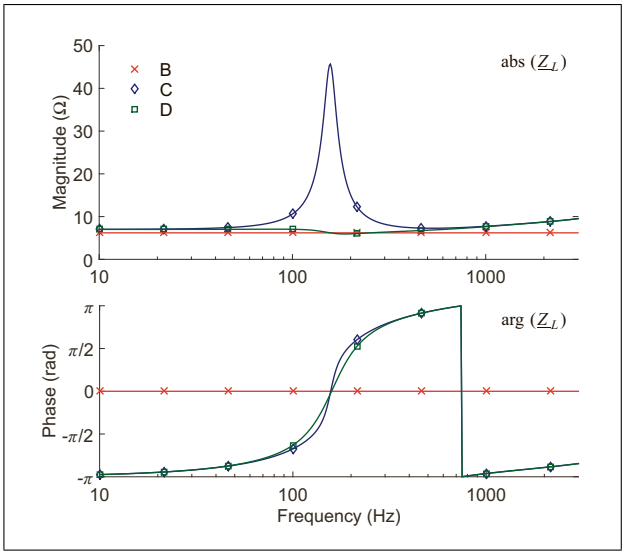

Figure 4. Target frequency response of the electrical loads to be synthesized, after Equation (9).

ure 4 shows the frequency response function of the electrical impedances $\underline{Z}_L$ calculated from Equation (9) with the setting parameters listed in Table II.

3.2. Experimental setup

In order to check the validity of the SEA, a standing-wave duct was specifically designed (length $L = 1.5$ m and inner diameter $\phi = 75$ mm), one termination of which is closed by a SEA loaded by a rear enclosure of volume $V_b = 0.96\,\mathrm{dm}^3$. As depicted in Figure 5, the other end is closed by a sound source delivering a band-pass filtered broadband noise in the frequency range [20 Hz - 2 kHz]. Although this experimental setup is one-dimensional, it is intended to show the effect of the different synthetic electrical loads in the same experimental conditions, both in terms of sound absorption coefficient and attenuation of duct modes (presented in Section 3.5). This experimental setup is similar to those used in previous work [6, 8, 9, 12], allowing direct comparison. As can be seen in Figure 5, three holes located at positions $x_1 = 0.6$ m, $x_2 = 0.35$ m, and $x_3 = 0.26$ m from the EA are holding 1/2" microphones (Norsonic Type 1225 cartridges mounted on Norsonic Type 1201 amplifier), sensing the sound pressures $\underline{p}_1 = \underline{p}(x_1)$, $\underline{p}_2 = \underline{p}(x_2)$ and $\underline{p}_3 = \underline{p}(x_3)$. The transfer functions $\underline{H}_{13} = \underline{p}_3/\underline{p}_1$ and $\underline{H}_{23} = \underline{p}_3/\underline{p}_2$ are processed through a Pulse® Bruel and Kjaer multichannel analyser. This standing-wave duct allows assessing the normal incidence sound absorption coefficient of the SEA in the frequency range from 57 Hz to 1715 Hz. The displayed frequency range is limited to 1 kHz in the following in order to focus the analysis in the frequency range of interest.

3.3. Implementation of the synthetic electrical load

This section presents the mixed digital-analog approach used to practically implement the electrical admittances calculated from Equation (10) with the setting parameters given in Table II. First, a digital filter was calculated by converting Equation (10) to a linear constant-coefficient difference equation using the z-transform. Then, the filter coefficients corresponding to the desired specifications were implemented on a digital platform. In this study, digital processing was performed using a National Instrument CompactRIO® real-time Field Programmable Gate Array

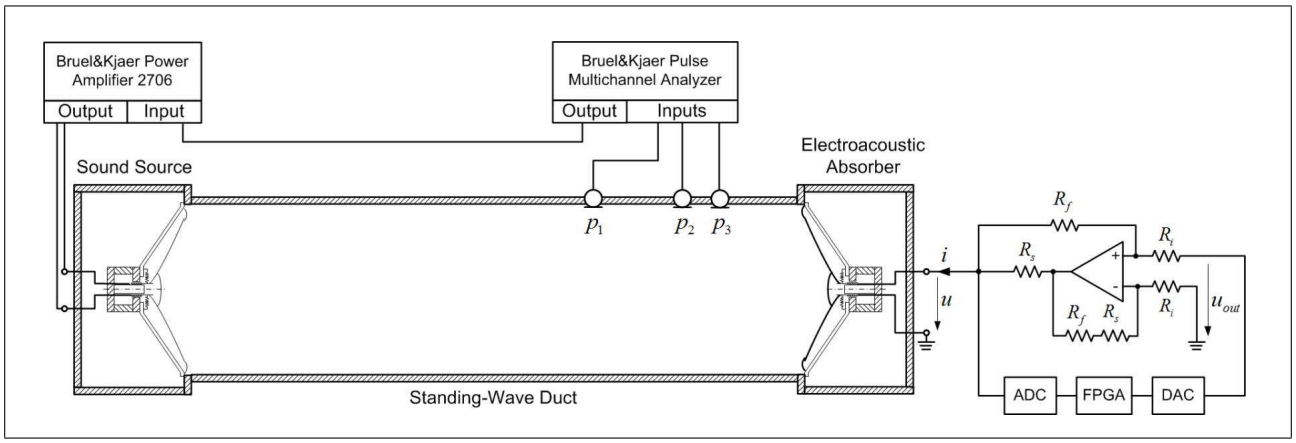

Figure 5. Scheme of the experimental setup.

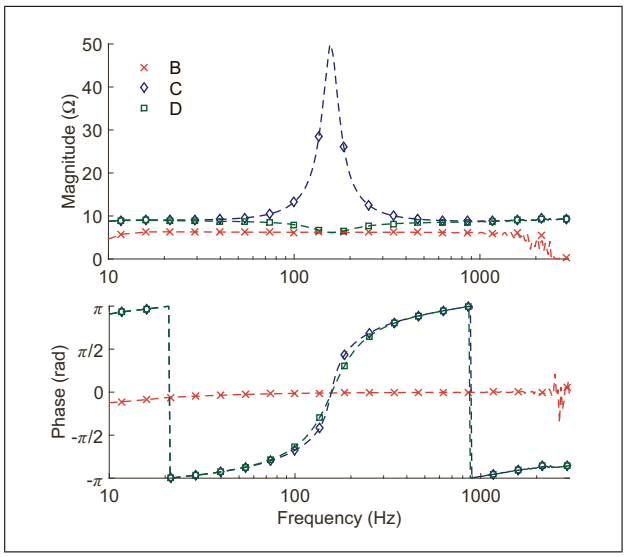

Figure 6. Electrical impedance measured at the SEA input terminals (i.e. from $\frac{u}{i}$ in Figure 5). The corresponding control settings can be found in Table II.

(FPGA) module. The NI 9215 module (± 10 V dynamic range, 16-bit resolution) was used for data acquisition and the NI 9263 module (± 10 V output range, 16-bit resolution) was used for analog output. As illustrated on the right-hand side of Figure 5, the input signal u of the filter is the voltage sensed at the transducer terminals which is then sampled by the analog to digital (AD) converter. After digital processing, the filtered signal u_{out} is converted into an output current so that the synthetic load is "seen" as an electrical admittance at the loudspeaker input terminals. As shown in Figure 5, the voltage-controlled current source is basically an op-amp based "improved" Howland current pump circuit including an operational amplifier, two input resistors R_i, two feedback resistors R_f and a current sense resistor R_s. More details about the design of the circuit can be found in [21].

Figure 6 shows the measured electrical impedances presented by the digital-analog synthetic load, designed with the setting parameters given Table II. In practice, this measurement was performed when the SEA is subject to an external broadband stationary noise produced by the opposite sound source. As can be seen in Figures 4 and 6, there is a good agreement between the analytical model and the measured shunt electrical admittances. The amplitude measured in case B (equivalent to the connection of a resistor at the input terminals) starts decreasing above 1 kHz, which might be due to the fact that the output voltage u at the transducer terminals is too small in this frequency range for the level of excitation of the sound source [3]. In cases C and D, however, the synthetic electrical admittance is complex and frequency dependent, and resistive only around the loudspeaker resonance frequency.

3.4. Measured acoustic performance

The specific acoustic impedance and sound absorption coefficient were assessed according to ISO 10534-2 standard [22]. Figure 7 illustrates the measured acoustic performance of the SEA when the synthetic electrical loads depicted in Figure 6 are connected to the input terminals. When connecting a resistor across the input terminals, the effective resistance of the diaphragm is changed but not the overall reactance (see. Figure 7, case B). As expected, the diaphragm specific acoustic impedance can be matched to the characteristic impedance of air but only around the SEA resonant frequency, leading to a maximum absorption coefficient $\alpha = 1$ as illustrated on the right-hand side of Figure 7. The resistance and reactance of the diaphragm impedance can be changed by connecting the synthetic electrical loads, as can be seen in Figure 7. Compared to cases A or B, the slope of the imaginary part in cases C and D is lower, showing that the reactance of the diaphragm impedance is actually reduced. In case D in particular, the specific acoustic resistance may be relatively well matched to the characteristic impedance of air, i.e. $\rho c \simeq 414\ \mathrm{N\,s\,m^{-3}}$, while decreasing both the effective mass and compliance of the diaphragm, leading to an increased bandwidth. To target a 90% absorption as in

[3] the output voltage of the Pulse® sound generator is set so that the average sound pressure amplitude is about 1 Pa at the microphone positions.

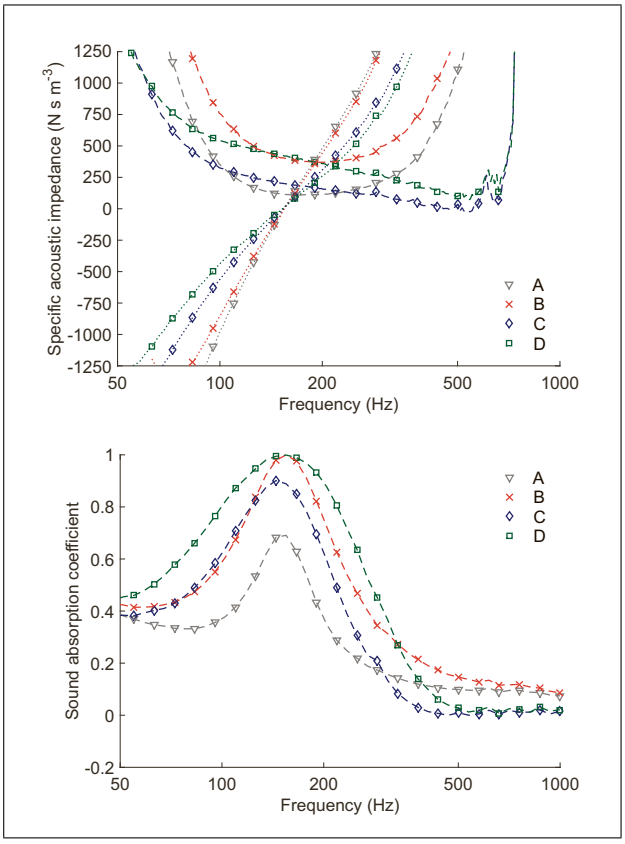

Figure 7. Real part (- - -) and imaginary part (· · ·) of the specific acoustic impedance (top) and corresponding sound absorption coefficient (bottom) measured at the diaphragm of the SEA for normal sound incidence.

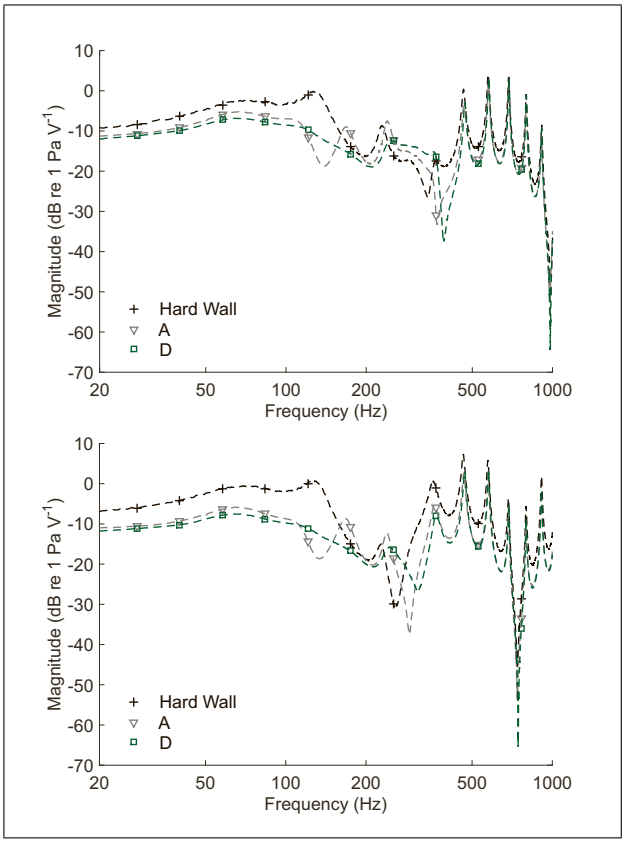

Figure 8. Sound pressure level measured at 0.26 m (top) and 0.35 m (bottom) from the duct termination with a hard surface panel, the loudspeaker in open circuit (A) and shunted with a synthetic electrical admittance (D).

case C, for example, the specific acoustic resistance should be set at approximately half the characteristic impedance value, while slightly decreasing the reactance of the diaphragm impedance, as illustrated on the right-hand side of Figure 7. This experimental result clearly shows that a shunt electrical admittance can be tailored so that a conventional loudspeaker can be turned into a SEA over a broader frequency range than can offer a simple shunt resistor.

3.5. Damping of low-frequency modes in a duct

In this section, the SEA examined in Section 2 is used for damping the low-frequency modes in a duct. For the purpose of illustration, the experimental setup is the same as that described in Section 3.2.

Figure 8 shows the sound pressure level measured at two different locations in the duct (at 0.26 m and 0.35 m away from the SEA), in three configurations. In the configuration "hard wall", a hard surface panel was substituted for the SEA at the duct termination; in case A, the duct was ended by the SEA in open circuit (without control) and in case D a synthetic electrical load was connected to the SEA with a view to achieving ideal impedance matching (see Table II). As shown in Figure 8, the peaks (resonances) and the dips (anti-resonances) in the duct are significantly attenuated using the SEA connected to the synthetic electrical load. Compared to the hard wall case, the dynamic range of the sound pressure level in the duct is reduced by 15 dB between 50 Hz and 300 Hz (31.9 dB between peak and dip versus 17 dB in case D). As can be seen in Figure 8, the bandwidth of efficient attenuation is clearly larger when a synthetic load is used compared to the loudspeaker in open circuit (case A). This clearly shows the capability of the SEA to achieve sound absorption at the duct termination, allowing to flatten the low-frequency frequency response all along the duct. Note that duct modes above 400 Hz could be attenuated with conventional absorbing materials such as microperforated panels or porous layers, without affecting the performance of the SEA, thus improving the overall absorption performance as suggested in [23, 24].

4. Discussions

As confirmed experimentally in Section 3, a complex, frequency-dependent electrical load can be derived from the loudspeaker model to improve the sound absorption capability of its diaphragm, thus creating a sensorless electroacoustic absorber (SEA). With our mock-up SEA prototype based on a commercially available electrodynamic loudspeaker, the bandwidth of efficient sound absorption ($\alpha \geq 0.83$) already spans in the frequency range from

100 Hz to 210 Hz, which is larger than what can be obtained using a simple resistor.

The working range of the SEA is mainly limited by the characteristics of the loudspeaker driver and the non-ideal behaviour of some of its components. As shown in Equations (7) and (9), the function of the synthetic electrical load is actually to increase the overall resistance and decrease the overall reactance of the specific acoustic impedance of the loudspeaker diaphragm. This makes it clear that the expected results in this case will be around the loudspeaker resonance frequency. On the other hand, the overall acoustic performance and stability of the SEA are sensitive to model uncertainties in the loudspeaker system. Limiting factors to the higher frequencies are due to frequency-dependent variations of certain components of the loudspeaker that are not taken into account in our basic model. As can be seen in Equation (9), the derivation of the synthetic electrical load means that the blocked electrical impedance must be cancelled, which can hardly be achieved perfectly in practice [6, 14]. Discrepancies between the lumped parameter model and the actual electrodynamic driver are described in the literature [15, 18, 27, 28]. In particular, the non-ideal behaviour of the voice coil transducer from which the SEA is developed might be significant. It is recognized that eddy currents may modify the loudspeaker electrical impedance [15, 27], making it difficult to cancel even when using a lossy inductance in the model. A second possible cause is related to the suspension creep [28], which is not covered by our simplified model.

An expanded model accounting for suspension creep could be considered in future work with a view to further extending the working range of the SEA, or an ironless actuator could be designed in order to reduce the above-mentioned effects. Note that if high levels of excitation are assumed, some of the model parameters would need to be considered as time-varying nonlinear functions of the input variables [15, 16].

Unlike previous attempts to achieve broadband impedance matching using a purely analog network [6], the mixed digital-analog approach proposed in this study allows more flexibility to refine the synthetic admittance coefficients, making it less sensitive to mismatches in the loudspeaker model. The frequency response of the voltage-controlled current source used to implement the synthetic electrical loads is likely to have high-frequency variations when connected to the loudspeaker due to the self inductance of the coil.

For a successful implementation, any parasitic phase shift in the current source must be taken into consideration at the design stage of digital filters, and a compromise has to be found between high loop gain to achieve good performance in the frequency range of interest and low gain to ensure stability outside the working frequency range. To that purpose, it may be helpful to employ phase compensators [12] in order to improve the closed-loop stability. On the other hand, the latency in digital processing, not accounted for in the analytical model, is also a limiting factor. Therefore, direct AD/DA converters were preferred to sigma-delta converters as they have a lower latency [4]. A high sampling rate can be advantageous in terms of latency in the AD/DA converters, but it also means that high-frequency noise is more likely to be captured in the signal, which can also affect the overall performance of the SEA. Likewise, no anti-aliasing and reconstruction filters were used in order to optimize the response time of the controller. Note that a FPGA platform was used here, but other digital platforms such as micro-controllers or digital signal processor s (DSP) may obviously be used as well.

Compared to previous work on the design of a synthetic electrical admittance to control resonant sound fields, the sensitivity to changes in sound field or the location of the control loudspeaker is no longer relevant. In [8] for example, the problem is tackled from a feedback control perspective by using optimal $\mathcal{H}_\infty$ and $\mathcal{H}_2$ controller to obtain the optimal electrical admittance. The approach developed in [8] consists basically in solving an optimal problem on a system comprising the loudspeaker and the duct. It results from the above that the synthetic load is only effective for a given location of the loudspeaker in the duct and is not robust as no adaptation can be applied. With the approach developed in the present paper, the synthetic load is designed to achieve impedance matching at the loudspeaker diaphragm, i.e. regardless of the sound field in which the SEA is located. Through this model-based approach, the shunt electrical admittance has also a straightforward physical interpretation regarding the control objective and can be set by adjusting the filter coefficients.

The results shown above were obtained for a 1D sound field in order to allow a straightforward comparison with previous work [6, 8, 9, 12]. Nevertheless, extension to 3D sound fields is possible. It was shown in [9] that the behaviour of electroacoustic absorbers observed in a waveguide was still valid when disposed in actual lightly damped rooms. Further experiments even showed that the SEAs can be arranged either in array (close to each others) or disposed individually in the corners of the room, at a more or less arbitrary location in the room without compromising the overall acoustic performance. This shows the potential of SEAs to attenuate low-frequency modes in listening rooms, such as home-theaters or recording studios, since it might improve the quality of sound reproduction by flattening the frequency response of the music sources. The SEAs are also attractive compared to conventional bass traps in terms of bandwidth and compactness. In addition, SEAs stand out for their versatility because the diaphragm specific impedance can be set by adjusting the filter coefficients of the synthetic load admittance. However, it can be argued that the target acoustic impedances to be achieved may also be optimized by taking into account additional parameters such as the wall impedance and the ratio of effective piston area of the SEAs over the total surface area of wall, as discussed in [26].

[4] In this experiment we used a 50 kSPS sampling rate with a measured time delay of 23.8 μs (corresponding to 8.6^o phase shift per kHz).

5. Conclusions

This article presents a straightforward approach that can turn a conventional loudspeaker into a relatively broadband electroacoustic absorber. It is shown that a shunt electrical admittance can be designed so that the loudspeaker diaphragm is matched to a target specific acoustic impedance, regardless of the sound field in which the loudspeaker is located. In practice, a digital filter is used to replicate the target frequency response of the synthetic load, and a voltage-controlled current source is needed so that the filter is seen as an electrical admittance. Unlike previous attempts to implement the synthetic load using an electrical network, greater flexibility and accuracy can be obtained through this mixed digital-analog technology. With the SEA prototype based on a commercially available electrodynamic loudspeaker, the bandwidth of efficient sound absorption ($\alpha \geq 0.83$) ranges from 100 Hz to 210 Hz. The experiments confirmed the validity of SEA, showing that the dynamic range of the sound pressure level in the duct can be reduced by 15 dB from 50 Hz to 300 Hz compared to a hard surface panel. Even if the results are presented in a waveguide for normal incident sound wave, the method is still valid in actual rooms. The target specific acoustic impedance to be implemented may be more complex because it will depend on the wall impedance and the ratio of effective piston area of the SEAs on the total area of the wall.

Acknowledgement

This work was supported by the Swiss National Science Foundation (SNSF), under grant agreement 200020-132869.

References

[1] H. Kuttruff: Room acoustics. Spon Press, 5^{th} ed., 2009, 83-85.

[2] T. J. Cox, P. D'Antonio: Acoustic absorbers and diffusers: Theory, design and application. Taylor and Francis, 2^{nd} ed., 2009, Chap. 1, 14-16.

[3] B. M. Fazenda, M. Stephenson, A. Goldberg: Perceptual thresholds for the effects of room modes as a function of modal decay. J. Acoust. Soc. Amer. **137** (2015) 1088-1098.

[4] M. R. Avis, B. M. Fazenda, W. J. Davies: Thresholds of detection for changes to the Q factor of low-frequency modes in listening rooms. J. Audio Eng. Soc. **55** (2007) 611-622.

[5] R. L. Clark, K. D. Frampton, D. G. Cole: Phase compensation for feedback control of enclosed sound field. J. Sound and Vib. **195** (1996) 701-718.

[6] H. Lissek, R. Boulandet, R. Fleury: Electroacoustic absorbers: bridging the gap between shunt loudspeakers and active sound absorption. J. Acoust. Soc. Amer. **129** (2011) 2968-2978.

[7] H. Lissek, R. Boulandet, E. Rivet: Optimization of electric shunt resonant circuits for electroacoustic absorbers. Acoustics 2012, Nantes, France, 2012.

[8] A. J. Fleming, D. Niederberger, S. O. R. Moheimani, M. Morari: Control of resonant acoustic sound fields by electrical shunting of a loudspeaker. IEEE Trans. Contr. Sys. Tech. **15** (2007) 689-703.

[9] R. Boulandet: Tunable electroacoustic resonators through active impedance control of loudspeakers. EPFL Doctoral thesis no. 5331, 2012.

[10] H. F. Olson, E. G. May: Electronic Sound Absorber. J. Acoust. Soc. Amer. **25** (1953) 1130-1136.

[11] M. Furstoss, D. Thenail, M.-A. Galland: Surface impedance control for sound absorption: direct and hybrid passive/active strategies. J. Sound and Vib. **203** (1997).

[12] R. Boulandet, H. Lissek: Toward broadband electroacoustic resonators through optimized feedback control strategies. J. Sound and Vibration. **333** (2014) 4810-4825.

[13] A. J. Fleming, S. Behrens, S. O. R. Moheimani: Synthesis and Implementation of Sensor-Less Active Shunt Controllers for Electromagnetically Actuated Systems. IEEE Trans. Contr. Syst. Tech. **13** (2005) 246-261.

[14] M. J. Turner, D. A. Wilson: The use of negative source impedance with moving coil loudspeaker drive units: an analysis and review. 122th AES Convention, Vienna, Austria, 2007, 7072.

[15] J. Vanderkooy: A model of loudspeaker driver impedance incorporating Eddy current in the pole structure. J. Audio Eng. Soc. **37** (1989) 119-128.

[16] W. Klippel: Nonlinear large-signal behavior of electrodynamic loudspeakers at low frequencies. J. Audio Eng. Soc. **40** (1992) 483-496.

[17] R. Mariani, S. Bellizzi, B. Cochelin, P. Herzog, P.O. Mattei: Toward an adjustable nonlinear low frequency acoustic absorber. J. Sound and Vibration **330** (2011) 5245 - 5258.

[18] X-P. Kong, F. Agerkvist, X-W. Zeng: Modeling of lossy inductance in moving-coil loudspeaker. Acta Acustica united with Acustica **101** (2015) 650-656.

[19] M. Rossi: Audio. Presses Polytechniques Universitaires Romandes, Lausanne, 2007, 536-539.

[20] U. Seidel, W. Klippel: Fast and accurate measurement of the linear transducer parameters. 110th AES Convention, Amsterdam, Netherlands, 2001, 5308.

[21] R. A. Pease: A comprehensive study of the Howland current pump. National Semiconductor **29** (2008).

[22] ISO 10534-2-1998 : Acoustics - Determination of sound absorption coefficient and impedance in impedance tubes - Part 2: Transfer-function method. ISO, Geneva, Switzerland, 1998.

[23] P. Cobo, A. Fernández, O. Doutres: Low-frequency absorption using a two-layer system with active control of input impedance. J. Acoust. Soc. Am. **114** (2003) 3211-3216.

[24] J. Tao, R. Jing, X. Qiu: Sound absorption of a finite microperforated panel backed by a shunted loudspeaker. J. Acoust. Soc. Am. **135** (2013) 231-238.

[25] H. Lissek, R. Boulandet, E. Rivet, I. Rigas: Assessment of active electroacoustic absorbers as low frequency modal damper in rooms. InterNoise 2012, New-York City, USA, 2012.

[26] S. Karkar, E. Rivet, H. Lissek, D. Strobino, A. Pittet, V. Adam, A. Roux: Electroacoustic absorbers for the low-frequency modal equalization of a room: what is the optimal target impedance for maximum modal damping, depending on the total area of absorbers? Forum Acusticum 2014, Krakow, Poland, 2014.

[27] W. M. Leach: Loudspeaker voice-coil inductance losses: circuit models, parameter estimation and effect on frequency response. J. Audio Eng. Soc. **50** (2002) 442-449.

[28] M. H. Knudsen and J. Grue Jensen: Low-frequency loudspeaker models that include suspension creep. J. Audio Eng. Soc. **41** (1992) 3-18.